EXPERIMENTAL ANALYSIS OF THE DAMAGE INFLUENCE REGION IN SMART STRUCTURES THROUGH LAMB WAVES METHODOLOGIES

Vitor Ramos Franco, vrfranco86@yahoo.com.br
Aldemir Aparecido Cavalini Junior, aacjunior@aluno.feis.unesp.br
Bruno Rodrigues de Sunti, brunodesunti@hotmail.com
Vicente Lopes Junior, vicente@dem.feis.unesp.br
GMSINT – Grupo de Materiais e Sistemas Inteligentes, Department of Mechanical Engineering, UNESP/FEIS - Faculdade de Engenharia de Ilha Solteira, Av. Brasil 56, Ilha Solteira, SP, Brazil, ZIP CODE 15385000, Phone Number: +55 18 3743 1000, Fax Number +55 18 3742-2735, www.dem.feis.unesp.br/gmsint

Abstract. *This work presents an experimental analysis of the damage influence region in an aluminum plate like structure using Lamb Waves methodology and Piezoelectric Material (PZT) as actuators and sensors. Lamb waves are a form of elastic perturbation that remains guided between two parallel free surfaces, such as the upper and lower surfaces of a plate, beam or shell. The use of piezoelectric materials, coupled on a plate surface, in the formation of Lamb waves for SHM, is an important field of study. When a PZT is coupled on a plate surface and used as actuator, it tends to contract or expand, depending on the polarity of the electric field applied on it. As the structure deforms, a movement of bending is induced on the surface and these waves spread along the plate. These waves are "felt" to other PZTs, now being used as sensors. When a wave propagates on the plate, it comes at a PZT sensor from different ways. One way is when the wave reaches the sensor directly, i.e. without obstacles in the way in which the wave spread. The other possible way is when the wave reaches the sensor after reflected in the contours or discontinuities in the surface (structural damage). With the various features about the received signal, and with the use of certain techniques of signal processing, these damages can be detect and, thus, it's possible to realize the correct action trying to avoid a total failure of the structure. In this context, the experimental tests were realized in an aluminum plate structure, in the free-free-free-free boundary condition with piezoelectric patches (PZT) coupled on its surface. One PZT patch was designated as actuator, exerting a predefined waveform into the structure. Then, another PZT became sensor and measured the response signals. The PZT actuator excited the structure at a frequency range of 30 to 35 kHz, in a sinusoidal waveform. The structural damage was simulated by additional masses coupled on the plate surface. The damages were placed in specific positions on the plate surface and the position of these damages was varied in order to obtain the influence region of the damage. It was used four damage indexes to detect structural damages using the Lamb Waves methodology: Root-Means-Square Deviation (RMSD), Metric Damage Index (MDI), H_2 Norm and Correlation Coefficient Deviation (CCDM). These indexes were computed in frequency domain considering the Frequency Response Function (FRF) of the output signals. The indexes showed the difference when a damaged structure was considered. With the results obtained, it's possible to obtain the region in which the damage can be detected and making the correct Structural Health Monitoring scheme through Lamb Waves methodologies using piezoelectric materials as actuators and sensors.*

Keywords*: Structural Health Monitoring, Lamb Waves, Piezoelectric Material, Frequency Domain*

1. INTRODUCTION

Nowadays, in the world of engineering, there is an interest in the development of a real-time Structural Health Monitoring (SHM) method. SHM is a system with the ability to detect and interpret adverse "changes" in a structure. An SHM system examines the structure for damage and provides information about any damage that is detected. This type of system allows systems and structures to actively monitor their own structural integrity (Inman *et al*., 2005). An SHM system typically consists of an onboard network of sensors for data acquisition and a central processor to evaluate the structural health. The development of "smart structures" has provided the necessary technology to implement in-situ monitoring systems into complex structures. With the advances in actuator technology, particularly collocated sensor-actuators, and microcomputer processing, effective and inexpensive Non-Destructive Evaluation of large complex structures can be developed. The concept of the structural integration of sensing is known as "an intelligent system" or "a smart structure". To be effective, a SHM system must provide real-time and continuous structural health assessment. The sensors must be an integral part of the structure, i.e., in-situ, in order to provide a measurement on a continuous basis (Castanien and Lian, 1996).

Considered among the most promising methods in structural dynamics for SHM, the method of interrogating a structure with high frequency waves (Lamb waves) is investigated in this paper. Many researchers have studied the technology of SHM in which piezoelectric sensors/actuators are integrated into a structure. Using these actuators and sensors it is possible to realize a structural monitoring system using Lamb waves. In particular, the use of Lamb waves can offer a way of estimating damage occurrence in a structure in terms of location, severity and type of damage. Several different applications can be cited in this area, for instance, Franco *et al.* (2009) used piezoelectric material for

detecting and locating damages in plate-like structures. A set of PZT patches were attached to the plate surface so that they could generate Lamb waves and make a configuration that it was possible to locate the damage with accuracy. Damage Indices obtained from experimental data involving the Frequency Response Function were computed from the output signals measured using different combination of piezoelectric actuator/sensor pairs. The results showed the viability of the presented methodology to damage location in smart structures.

As a result of the varying challenges offered by different structures and systems, significant research effort has been applied to SHM with the emergence of a broad range of techniques, algorithms and methods. Rytter (1993) classified the various methods based on the level of the identification:

- Level 1: Determination that damage is present in the structure;
- Level 2: Determination of the geometric location of the damage;
- Level 3: Quantification of the severity of the damage;
- Level 4: Prediction of the remaining service life of the structure.

In this context, this paper presents an experimental SHM technique using the level 1 described above. In order to illustrate the results an experimental test-bed involving a plate structure was used. Two PZT patches were configured as actuator and sensor, generating and sensing Lamb waves, in a certain way that was possible to find the damage influence region. Structural damage was simulated by adding small masses to the plate in specific regions on the plate surface. Four damage indices were used: Root-Mean-Square Deviation (RMSD), Metric Damage Index (MDI), Coefficient Correlation Deviation Mean (CCDM) and H_2 Norm, all of them computed in the frequency domain, using the Frequency Response Function (FRF) of the output signals. With the configuration done in the plate surface, it was possible to find the region in which the damage can be located (damage influence region) using Lamb waves approach.

1. DESCRIPTION OF LAMB WAVES

Lamb waves are a form of elastic perturbation that remains guided between two parallel free surfaces, such as the upper and lower surfaces of a plate, beam or shell. This type of wave phenomenon was first described by Horace Lamb in 1917; however, he never attempted to produce them (Kessler *et al.*, 2002). There are two groups of waves, symmetric (S) and anti-symmetric (A), that satisfy the wave equation and boundary conditions for this problem and each can propagate independently of the other. The symmetric group is used for damage detection in metallic structures and the anti-symmetric one is used for damage detection in composites structures. The present work utilizes PZT patches to excite the first symmetric Lamb wave mode. Lamb waves are formed when the actuator excites the structure's surface with a pulse after receiving a signal.

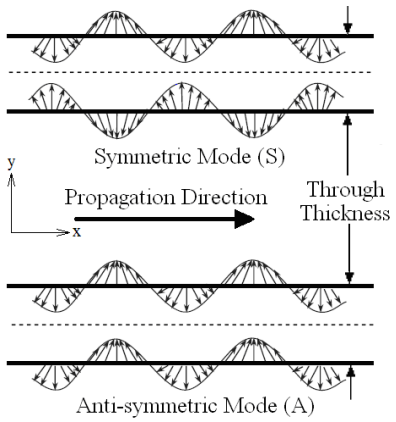

Figure 1. Graphical representation of S and A Lamb wave shapes.

The theory of Lamb waves is fully documented in a number of textbooks. Here, it's only reproduced an overview (Inman *et al.*, 2005). The analysis starts with the Helmholtz decomposition that considers the decomposition of Navier's elastodynamic vector equation

$$(\lambda+\mu)\nabla\nabla\cdot\mathrm{u}+\mu\nabla^2\mathrm{u}=\rho\ddot{\mathrm{u}} \tag{1}$$

Letting the displacement vector **u** be expressed as

$$\mathbf{u}=\nabla\phi+\nabla\times\psi \tag{2}$$

into a scalar wave equation and a vector wave equation, given by

$$\nabla^2\phi = \frac{1}{c_L{}^2}\ddot{\phi}\ ,\ \nabla^2\psi = \frac{1}{c_T{}^2}\ddot{\psi} \tag{3}$$

where ϕ and ψ are two potential functions,

$$c_L^2 = \frac{(\lambda+2\mu)}{\rho},\ \ c_T^2 = \frac{\mu}{\rho} \tag{4}$$

are the pressure (longitudinal) and shear (transverse) wavespeeds respectively, ρ is the mass density,

$$\mu = \frac{E}{2(1+v)},\ \ \lambda = \frac{Ev}{(1-2v)(1+v)} \tag{5}$$

are the Lamé's constants, *E* is the Young's modulus and *v* is the Poisson ratio.

Now, consider an infinite plate of thickness 2d, i.e. the domain $\Omega = \{(x, y, z) = (-\infty,\infty)\times(-\mathrm{d},\mathrm{d})\times(-\infty,\infty)\}$ with free surfaces (Fig. 2). Waves in the interest are in the x-y plane, and there are no variations along z, i.e. $\partial/\partial z = 0$.

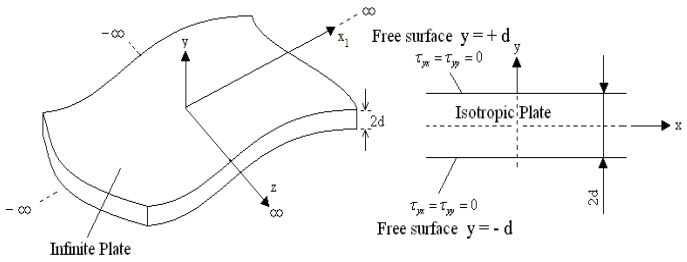

Figure 2. Infinite plate with free surfaces

For this case, the Helmholtz's decomposition yields (Inman *et al.*, 2005):

$$\begin{aligned} u_x &= \frac{\partial\phi}{\partial x} + \frac{\partial\psi_z}{\partial y},\ u_y = \frac{\partial\phi}{\partial y} - \frac{\partial\psi_z}{\partial x} \\ u_z &= -\frac{\partial\psi}{\partial y} + \frac{\partial\psi_y}{\partial x}\ ,\ \frac{\partial\psi_x}{\partial x} + \frac{\partial\psi_y}{\partial y} = 0 \end{aligned} \tag{6}$$

Since the boundaries *y*=+d and *y*=-d are stress free, one has:

$$\tau_{yy} = 0\ ,\ \tau_{xy} = \tau_{yx} = 0\ ,\ \tau_{yz} = \tau_{zy} = 0 \tag{7}$$

in $y = \pm d$.

To derive the equations for Lamb waves, consider first the governing equations in terms of Helmholtz scalar and vector potentials, Eq. 3. Seeking plane wave solutions in the x-y plane for waves propagating along the +x direction, assume solutions of the form:

$$\begin{aligned} \phi &= (A_1 \sin py + A_2 \cos py)e^{i(\xi x-\omega t)} \\ \psi &= (B_1 \sin qy + B_2 \cos qy)e^{i(\xi x-\omega t)} \end{aligned} \tag{8}$$

where $\xi = \omega/\mathrm{c}$ is the wavenumber and

$$p^2 = \frac{\omega^2}{c_L^2} - \xi^2, \quad q^2 = \frac{\omega^2}{c_T^2} - \xi^2 \tag{9}$$

The four integration constants, A_1, A_2, B_1, B_2, are found from the boundary conditions. Thus, two possible solutions result:

$$\begin{aligned} D_S &= (\xi^2 - q^2)^2 \cos pd \sin qd + 4\xi^2 pq \sin pd \cos qd = 0 \\ D_A &= (\xi^2 - q^2)^2 \sin pd \cos qd + 4\xi^2 pq \cos pd \sin qd = 0 \end{aligned} \tag{10}$$

representing the symmetric and anti-symmetric motion respectively.

Equation 10 can be rewritten in the more compact form as the Rayleigh–Lamb equation:

$$\frac{\tan qd}{\tan pd} = \left[\frac{-4pq\xi^2}{(\xi^2 - q^2)^2} \right]^{\pm 1} \tag{11}$$

where +1 corresponds to symmetric (S) motion and -1 to anti-symmetric (A) motion.

Therefore, given a certain isotropic material, Eq. 11 can be solved numerically to find the relation between the driving frequency ω and the wavenumber ξ from which the corresponding phase velocity $c_p = \omega / \xi$ can be found.

3. DAMAGE-SENSITIVE INDEXES

Three indices obtained through the FRF were investigated in this paper.

3.1. Root-Mean-Square Deviation (RMSD)

The RMSD index is presented here in the following form (Lopes Jr *et al.*, 2002):

$$RMSD = \sum_{i=1}^{n} \sqrt{\frac{\left[\left(Y_{i,1}\right) - \left(Y_{i,2}\right)\right]^2}{\left[\left(Y_{i,1}\right)\right]^2}} \tag{12}$$

where $Y_{i,1}$ is the FRF of the baseline condition, or healthy structure, of the PZT sensor and $Y_{i,1}$ is the FRF in the same PZT in unknown structural conditions at frequency interval i.

3.2. H_2 Norm

The H_2 norm of a system is used to characterize the system itself, along with its modes and its sensors. Let $G(\omega)$ be a transfer function of a system. The H_2 norm of the system is defined as (Gawronski, 1998):

$$\|G\|_2^2 = \frac{1}{2\pi} \int_{-\infty}^{+\infty} \mathrm{tr}\left(G^*(\omega)(G(\omega))\right) d\omega \tag{13}$$

where tr is the trace of $G*(\omega)(G(\omega))d\omega$.

Generally, the H_2 norm is computed using modal coordinates, but in this way it is necessary to obtain a model for the equation motion. The numerical value for the H_2 norm for a SISO (single-input-single-output) system corresponds the area under the absolute value of the FRF of the system (Gawronski, 1998). In this paper, the area under of the FRF curve was computed using the Trapezoidal method, implemented in the software Matlab® through command "trapz" (Bueno *et al.*, 2007).

The H_2 norm can be used for damage detection using the following procedure: consider the norm computed using the j*th* PZT sensor; and denoting it for a healthy structure by $\|G_{shj}\|_2$, and j*th* PZT sensor norm of a damaged structure by $\|G_{sdj}\|_2$. The j*th* sensor index of the structural damage is defined as weighted difference between the j*th* sensor norm of healthy and unknown structural conditions (damaged structure) (Gawronski and Sawicki, 2000):

$$H_{2sj} = \frac{\left| \left\| G_{shj} \right\|_2^2 - \left\| G_{sdj} \right\|_2^2 \right|}{\left\| G_{shj} \right\|_2^2} \tag{14}$$

where H_{2sj} is the H_2 Norm index, $j = 1,\ldots, r$; and r is the PZT sensor number. Note that the sensor index reflects the impact of the structural damage on the j*th* sensor.

3.3. Metric Damage Index (MDI)

The Metric Damage index that supplies an estimate of the structural variation, is calculated using the following equation

$$MDI = \sum_{i=1}^{n} \left[\left(Y_{i,1} \right) - \left(Y_{i,2} \right) \right]^2 \tag{15}$$

where MDI is the Metric Damage index, $Y_{i,1}$ is the FRF magnitude measured in the structure before the damage (baseline condition), $Y_{i,2}$ is FRF magnitude measured in the structure in normal operation conditions (unknown structural conditions) at frequency interval i (Park *et al.*, 2000).

3.4. Correlation Coefficient Deviation Mean (CCDM):

The CCDM is closely related to the RMSD and is given by:

$$CCDM = 1 - r = 1 - \frac{\mathbf{cov}\left(Y_{i,1}, Y_{i,2}\right)}{S_{Y_1} S_{Y_2}} = 1 - \frac{1}{n-1} \frac{\sum_{i=1}^{n} \left(Y_{i,1} - \overline{Y}_1\right)\left(Y_{i,2} - \overline{Y}_2\right)}{S_{Y_1} S_{Y_2}} \tag{16}$$

where r is the correlation coefficient, **cov** is the cross-covariance and S is relative to the sample standard deviation. $Y_{i,1}$ is the FRF magnitude measured in the structure before the damage (baseline condition), $Y_{i,2}$ is FRF magnitude measured in the structure in normal operation conditions (unknown structural conditions) at frequency interval i. Here r is the value that indicates how well the baseline (reference signal) and the measurements in the unknown conditions are linearly related. Thus, high values are expressive that the data are uncorrelated, or else, there is a variation, probably occurred due to the damage.

4. EXPERIMENTAL METHODOLOGY

The experimental tests were performed in an aluminum plate-like structure, in the free-free-free-free boundary condition, with four PZTs attached on its surface (Fig. 3a). Figure 3b shows the detail of PZTs used in the formation of the Lamb waves. The plate properties and dimensions are shown in table (1).

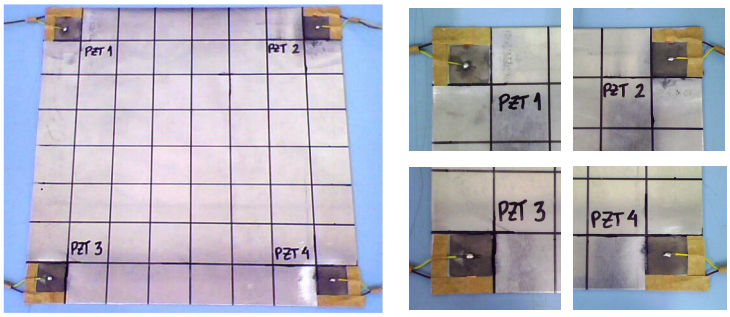

(a) (b)

Figure 3. (a) Aluminum Plate (b) Detail of the PZTs.

Table 1. Physical properties and dimensions of the plate.

Property	Value
Young Modulus (GPa)	70
Thickness (m)	0.0015
Length/Width (m)	0.24
Density (Kg/m^3)	2710

The PZT 2 was designated as actuator, sending a predefined wave through the structure's surface and the PZT 3 became sensor and measured the response signal. The experimental setup is shown in Fig. 4a and the scheme input/output is shown in Fig. 4b.

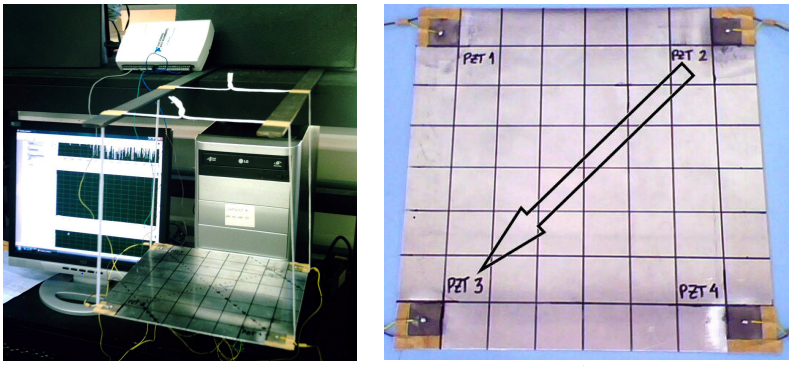

(a) (b)

Figure 4. (a) Experimental Setup; (b) Excitement and Measurement Procedure.

In order to find the damage influence region through Lamb waves methodology, it was necessary to make a specific configuration that is able to show the boundary region between the PZT actuator and sensor in which the damage can be detected. For this, a line was drawn diagonally across the plate, joining the PZT 2 (actuator) and PZT 3 (sensor), referred to "center line". Perpendicular to this line, three other lines were drawn, as can be seen in Fig. 5:

- The first line was drawn closer to PZT 2 (actuator).
- The second line was drawn in the central region of the plate (the other diagonal of the plate, joining the PZT 1 and PZT 4).
- The third line was drawn closer to PZT 3 (sensor).

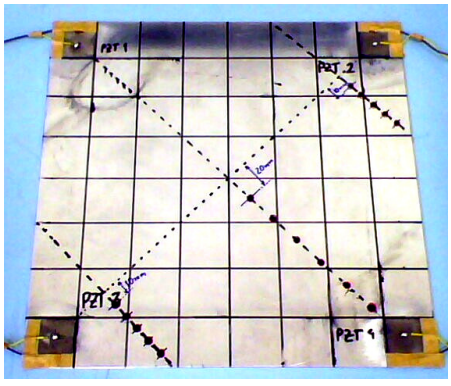

Figure 5. Configuration Drown in the Plate Surface.

In each line, marks were made in which the damages were positioned. Whereas there is symmetry of the wave on the "central line", the tests were performed with the damage being placed on only one side of the structure. In the first and third line, marks were made every 10 mm, from the center line, as seen in Fig. 6a and 6c respectively. In the second line, in the central area, the marks were made every 20mm, Fig. 6b.

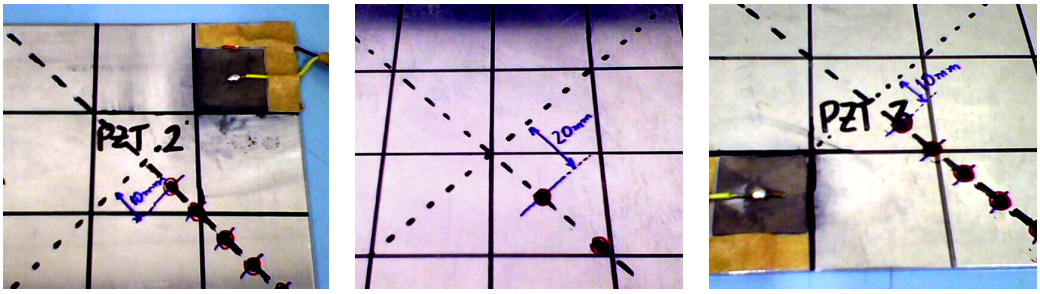

(a) (b) (c)

Figure 6. Detail of the lines drown (a) closer to PZT 2, (b) in the central region and (c) closer to PZT 3.

The PZT actuator excited the structure in a frequency range of 30 to 35 kHz, in a sinusoidal waveform, exciting the first symmetric Lamb wave mode. It was used the National Instrument NI USB-6211 for the data acquisition. Firstly, the tests were realized in the structure without the damage, getting the baseline condition. Then, another test was performed with the structure without damage, in order to compare with the baseline condition. The failure was simulated by an additional mass (nut of 1g) coupled on the structure's surface. Three sets of tests were performed, now with the addition of the damages according to the scheme previously described, i.e.,

- Condition 1) Proximity of PZT 2: the damage was positioned 10mm from the center line and the position was varied of 10 in 10mm up to 50mm;
- Condition 2) Central Region: the damage was positioned 20mm from the center line, and the position was varied of 20 in 20mm up to 120mm;
- Condition 3) Proximity of PZT 3: The damage was positioned 10mm from the center line and the position was varied of 10 in 10mm up to 50mm.

Figure 7 shows some examples of FRFs obtained for different damage condition in the frequency range of 30-35 kHz.

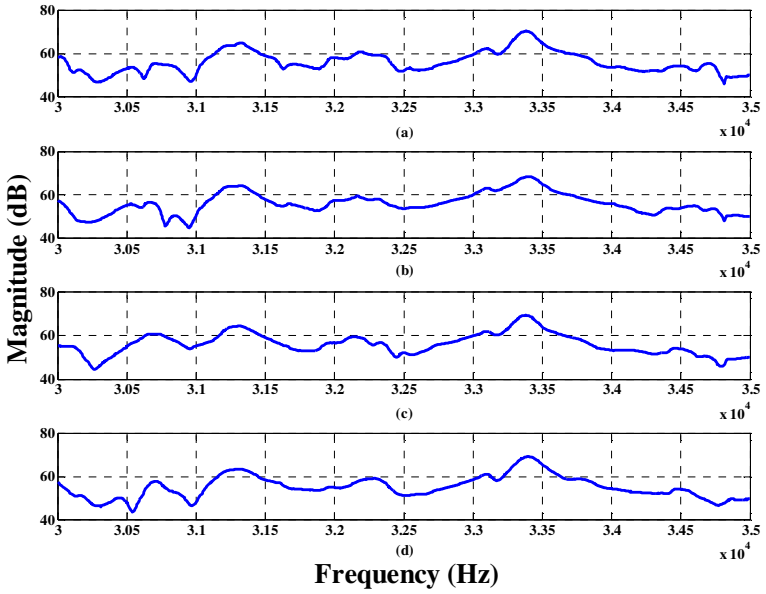

Figure 7. Examples of FRFs obtained in the experimental tests; (a) FRF – baseline, (b) FRF Condition 1 – 10mm, (c) FRF Condition 2 – 30mm, (d) FRF Condition 3 – 40mm.

Note that the FRFs have similar characteristics. With the FRFs of the output signals, four indexes were calculated for each damage condition. For the damage condition 1 (damage closer to the PZT 2), the following results were obtained.

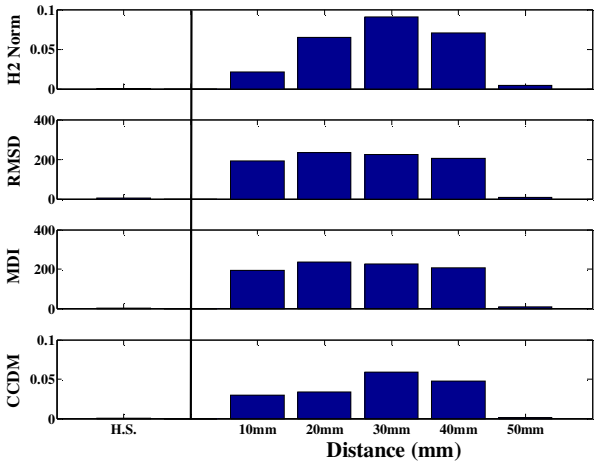

Figure 8. Damage Indexes computed to the Damage condition 1.

It is possible to observe in Fig. 8 that the indexes for the structure without the damage (referred to H.S.) were close to zero. When the damage was added to the structure in the 10mm position of the central line, all indexes were capable of to detect the presence of the damage in the structure. It is interesting to note that, as the damage go far to the center line, the indexes tend to rise in the beginning and after a certain position, the indexes do not detect the presence of damage anymore. For this damage condition, the damage is not detected when it is positioned at a distance of 50mm from the center line. Figure (9) shows the maximum position that the damage could be detected.

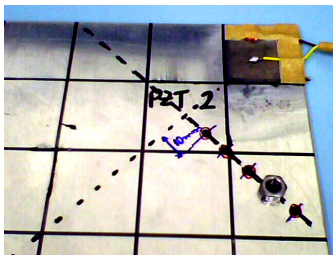

Figure 9. Maximum position of damage identification for the Condition 1.

Figure 10 shows the indexes obtained to the Condition 2.

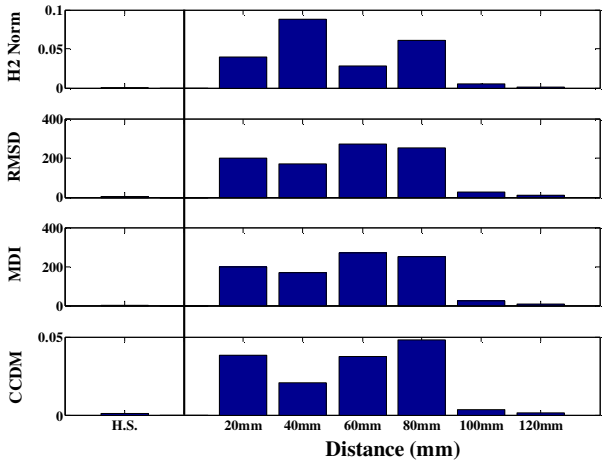

Figure 9. Damage Indexes computed to the Condition 2.

The four indexes for the structure without the damage (referred to H.S.) got values close to zero. However, when the damage was added in the 20mm position of the center line, all indexes were capable of to detect the presence of damage in the structure. Comparing to the previous Condition, note that the indexes tend to increase up to 80mm to the center line, and after that the indexes didn't detect the presence of the damage in the structure. Thus, it's possible to conclude that when the fault is in a position with a distance of approximately 100mm or more from the center line, the indices were not capable of to detect the damage anymore. Figure 11 shows the maximum position that the damage could be detected at the central region.

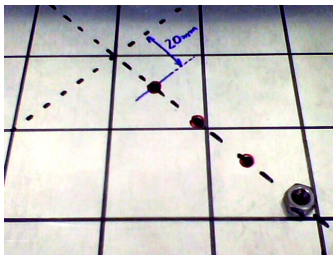

Figure 11. Maximum position of damage identification for the Damage Condition 2.

Figure 12 shows the indexes for the Condition 3.

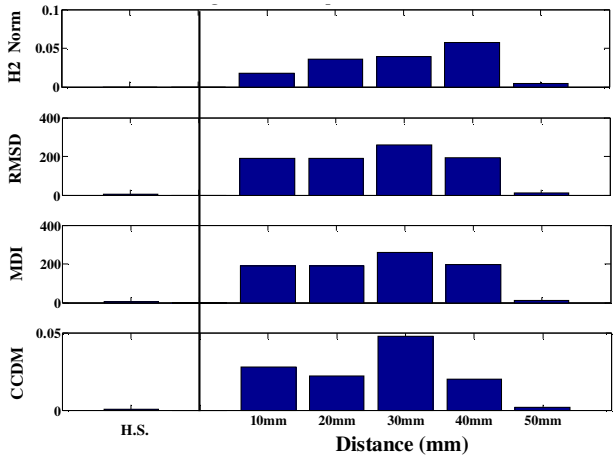

Figure 12. Damage Indexes computed to the Damage condition 3.

It's again possible to see that for the condition without the damage the indexes were close to zero. Note that the indexes have similar behavior to the Condition 1. Therefore, it is possible to conclude that for the Condition 1 and 3 the indexes are not able to detect the presence of the damage when the damage is at a distance of approximately 50mm or more from the center line. Figure 13 shows the maximum position that the failure could be detected in the proximities of PZT 3.

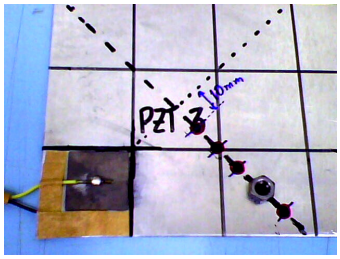

Figure 13. Maximum position of damage identification for the Condition 3.

With the previous obtained results, it is possible to identify the region where the damage can be detected through Lamb waves methodology. This region is shown in Fig. 14.

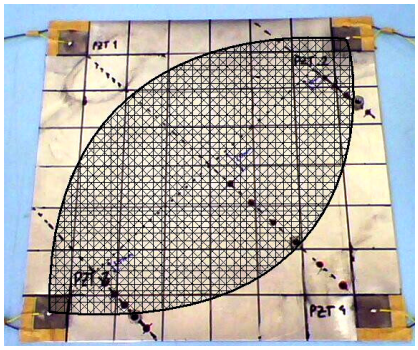

Figure 14. Damage Influence Region identified.

5. FINAL REMARKS

In this paper, four damage sensitive indexes were used to identify the damage influence region using the Lamb waves methodology. The indexes showed the difference when a damaged structure was considered. Generally, the indexes showed a peculiar characteristic: the indexes tend to increase when the failure go far from the center line until a certain point that the indexes began to decline up to the damage could not be detected anymore. Thus, the configuration used was capable of to identify the region where the damage can be detected.

6. ACKNOWLEDGEMENTS

The authors are thankful to CAPES, CNPq and to the members of GMSINT – **G**roup of **INT**elligent **M**aterials and **S**ystems.

4. REFERENCES

Bueno, D.D., Silva, S., Marqui, C.R. and Lopes Jr., V.,2007, "Compartive Study of Damage-Sensitive Indices Used for Structural Health Monitoring of Smart Structures", in 19th International Congress of Mechanical Engineering - COBEM, Brasília, DF.

Castanien, K. E. and Lian, C.,1996, "Application of active structural health monitoring technique to aircraft fuselage structures", SPIE: Smart Structures and Materials 1996, Vol 2721, pp. 38-49.

Franco, V. R., Bueno, Brennan, M.J., Cavalini Jr., Gonsalez, C.G. and Lopes Jr, V., 2009, "Experimental Damage Location in Smart Structures Using Lamb Waves Approaches", in 8th Brazilian Conference on Dynamics, Control and their Applications – DINCON 2009, Bauru, SP, Brazil.

Gawronski, W. K. and Sawicki, J.T., 2000, "Structural Damage Detection Using Modal Norms", Journal of Sound and Vibration, pp 194-198.

Gawronski, W.,1998, "Dynamics and Control of Structures, A Modal Approach", 1. Ed. New York, Springer Verlag.

Inman, D. J., Farrar, C. R., Lopes Jr., V. and Steffen Jr, V.,2005, "Damage Prognosis for Aerospace, Civil and Mechanical Systems." 01. ed. West Sussex: John Wiley & Sons Ltda, v. 01. 449 p.

Kessler, S. S., Spearing, S. M. and Soutis, C., 2002, "Damage detection in composite materials using Lamb wave methods" Smart Materials And Structures, 11, pp. 269–278.

Lopes Jr., V., Park, G., Cudney, H. H. and Inman, D. J., 2000, "Impedance based structural health monitoring with artificial neural networking". *Journal of Intelligent Material Systems and Structures*, v. 11, p. 206-214.

Park, G., Cudney, H. and Inman, D. J.,2000, "Impedance-based Health Monitoring of Civil Structural Components", ASCE/Journal of Infrastructure Systems, v. 6, n. 4, p. 153-160.

Rytter, A.,1993, Vibration based inspection of civil engineering structures. Ph.D. Dissertation, Department of Building Technology and Structural Engineering, Aalborg University, Denmark.

5. RESPONSIBILITY NOTICE

The authors are the only responsible for the printed material included in this paper.